



NRC Publications Archive Archives des publications du CNRC

Field tests of grouted rod anchors in permafrost Johnston, G. H.; Ladanyi, B.

This publication could be one of several versions: author's original, accepted manuscript or the publisher's version. /
La version de cette publication peut être l'une des suivantes : la version prépublication de l'auteur, la version
acceptée du manuscrit ou la version de l'éditeur.

Publisher's version / Version de l'éditeur:

Canadian Geotechnical Journal, 9, 2, pp. 176-194, 1972-10-01

NRC Publications Record / Notice d'Archives des publications de CNRC:

<https://nrc-publications.canada.ca/eng/view/object/?id=b9b09859-3a7b-490c-8580-2537dd6b826>;
<https://publications-cnrc.canada.ca/fra/voir/objet/?id=b9b09859-3a7b-490c-8580-2537dd6b8263>

Access and use of this website and the material on it are subject to the Terms and Conditions set forth at
<https://nrc-publications.canada.ca/eng/copyright>
READ THESE TERMS AND CONDITIONS CAREFULLY BEFORE USING THIS WEBSITE.

L'accès à ce site Web et l'utilisation de son contenu sont assujettis aux conditions présentées dans le site
<https://publications-cnrc.canada.ca/fra/droits>
LISEZ CES CONDITIONS ATTENTIVEMENT AVANT D'UTILISER CE SITE WEB.

Questions? Contact the NRC Publications Archive team at
PublicationsArchive-ArchivesPublications@nrc-cnrc.gc.ca. If you wish to email the authors directly, please see the
first page of the publication for their contact information.

Vous avez des questions? Nous pouvons vous aider. Pour communiquer directement avec un auteur, consultez la
première page de la revue dans laquelle son article a été publié afin de trouver ses coordonnées. Si vous n'arrivez
pas à les repérer, communiquez avec nous à PublicationsArchive-ArchivesPublications@nrc-cnrc.gc.ca.



Ser.
THI
N21r-2
no. 517

2273

NATIONAL RESEARCH COUNCIL OF CANADA
CONSEIL NATIONAL DE RECHERCHES DU CANADA

FIELD TESTS OF GROUTED ROD ANCHORS IN PERMAFROST

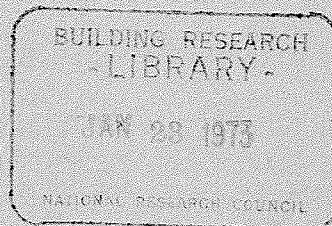
BY

G. H. JOHNSTON AND B. LADANYI

ANALYZED

Reprinted from
CANADIAN GEOTECHNICAL JOURNAL
Vol. 9, No. 2, May 1972
p. 176-194

49624



RESEARCH PAPER NO. 517
OF THE
DIVISION OF BUILDING RESEARCH

Price 25 cents

OTTAWA
October 1972

NRCC 12404

FIELD TESTS OF GROUTED ROD ANCHORS IN PERMAFROST

ABSTRACT

Field tests of grouted rod anchors installed in permafrost (frozen, stratified clays and silts containing ice at about 31.5 °F) at two test sites in northern Manitoba are described. The test program was undertaken to evaluate the resistance of frozen soils to uplift forces and, in particular, the time-dependent behaviour (creep) of frozen soil under load and the displacements associated with it. A theoretical analysis of the test results, based on engineering creep theory shows how the time-dependent behaviour of grouted rod anchors (or short piles) can be related to the basic creep parameters of frozen soil. In addition, it is shown how field creep data may be used for estimating long-term adfreeze strength of frozen soil of the design of anchors or piles.

ESSAIS SUR PLACE DES ANCRAGES A BARRES SCHELLES DANS LE PERGELISOL

SOMMAIRE

Des essais sur place des ancrages à barres scellées installées dans le pergélisol (argiles et limons gelés, et stratifiés contenant de la glace à 31.5 °F approx.) qui ont été faits sur deux sites situés dans le nord du Manitoba sont expliqués. Le programme des essais a été entrepris afin d'évaluer la résistance des sols gelés aux forces de soulèvement et, en particulier, le fluage du sol gelé sous la charge et les déplacements qui y sont associés. Une analyse théorique des résultats des essais basée sur une théorie de fluage d'ingénierie démontre comment le comportement des ancrages à barres scellées (ou pieux courts) peuvent être reliés aux paramètres fondamentaux de fluage du sol gelé. De plus, il est démontré comment des données de fluage sur place peuvent être utilisées pour calculer la force à long terme des adhésions du sol gelé pour le calcul des ancrages ou des pieux.

Field Tests of Grouted Rod Anchors in Permafrost¹

G. H. JOHNSTON

Division of Building Research, National Research Council of Canada, Ottawa, Canada, K1A 0R6

AND

B. LADANYI

Department of Mining Engineering, Ecole Polytechnique, Montreal, Québec.

Received August 16, 1971

Accepted January 4, 1972

Introduction

The use of guyed towers for power transmission and communication systems in northern Canada has received increased attention in recent years. In many cases perennially frozen ground (permafrost) poses special problems. The resistance of frozen soil to uplift forces must be evaluated for the design of anchors of guyed structures built on permafrost. There is little experience or information available, however, concerning the behavior of frozen soil in response to uplift forces or the capacity of various types of anchors. A field study of anchors in permafrost was therefore undertaken by the Division of Building Research of the National Research Council of Canada to evaluate, in particular, the displacements associated with long-term creep of frozen soil under load.

Initial appraisal of various kinds of anchors suggested that grouted rod anchors were a type that should be investigated. Early in 1967 a total of 18 such anchors (nine at each site) were installed in permafrost at Thompson and Gillam, Manitoba. This paper describes the installation and testing procedures and the results of the test programs conducted on the anchors at both sites.

In the analysis of the results the creep behavior of grouted anchors is related to basic creep parameters of frozen soil, taking into account the effects of temperature and normal pressure. The theory employed allows field creep data to be used for estimating the long-term adfreeze strength of frozen soil, information that is required in the design

of grouted rod anchors and piles. Estimated long-term adfreeze strengths were found to compare well with those observed by other investigators.

Description of Test Sites – Soils and Permafrost

Both Thompson and Gillam lie within the discontinuous permafrost zone in northern Manitoba (Fig. 1) where perennially frozen ground is found in islands or patches of variable thickness and areal extent. The occurrence of permafrost in this area is the result of a complex interrelation of climate and terrain factors so that the ground thermal regime is in a delicate state of equilibrium, with mean ground temperatures in frozen materials in the neighborhood of 31 °F. The test sites for the anchor studies were

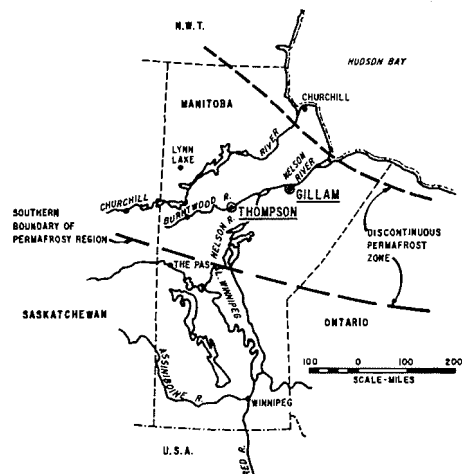


FIG. 1. Location of anchor test sites Thompson and Gillam, Manitoba.

¹Paper presented at the 24th Canadian Geotechnical Conference, Halifax, Nova Scotia, September, 1971.

selected on the basis of previous experience in both areas and after exploratory borings. Details of soil and permafrost conditions at each of the sites are given below.

Thompson

The test site is located in the SW corner (Fig. 2) of the Thompson townsite on the brow of a slope to the east of the Burntwood River. It is about 80 ft (24 m) above and 600 ft (183 m) from the river. The forest cover of very dense, stunted spruce and underbrush was machine cleared in early February 1967, care being taken to disturb the organic cover as little as possible.

In the Thompson area surficial deposits of stratified sediments (varved clays), laid down in glacial Lake Agassiz, overlie thinly stratified glacial drift consisting of a fine sandy gravel, a fine sand, or the Precambrian bedrock (Johnston *et al.* 1963). At the test site a borehole (TH-1) was drilled to a depth of 30 ft (9 m) on 8 March 1967. A 5 in. (13 cm) diameter flight auger was used to penetrate the hard-frozen material from ground surface to the 6 ft (2 m) depth; from 6 ft to 30 ft (2 m to 9 m) samples were taken continuously and undisturbed cores were obtained using

2 in. (5 cm) diameter heavy-wall Shelby tubes. The frozen cores were extruded and examined at the site and the occurrence and thickness of ice lenses and light and dark soil laminations recorded. Samples were taken for identification and classification. A thermocouple cable was installed in this hole to measure ground temperatures at 2 ft (.6 m) intervals from 2 to 20 ft (.6 m to 6 m) and at 25 and 30 ft (7.5 and 9 m) depths.

The soil profile, ice lens location and thickness, and pertinent information on the soils are shown in Figs. 3 and 4. The soil profile can be divided into two distinct strata. A varved clay of low to medium plasticity occurred to a depth of about 19 ft (6 m); this strata may be subdivided in two, based on thickness of the laminations. To 13 ft (4 m) the dark brown layers (clay) were from 1/2 to 1 in. (1 to 2.5 cm) thick and the light brown or tan colored layers (silt) increased in thickness with depth from 1 to 3 in. (2.5 to 7.5 cm). Between 13 and 19 ft (4 and 6 m) the dark layers were from 1/2 to 3/4 in. (1.2 to 1.9 cm) thick, but the silt layers were dominant, varying from 3 to 12 in. (7.6 to 30.5 cm) in thickness. From 19 to 30 ft (6 to 9 m) the soil was a tan colored,

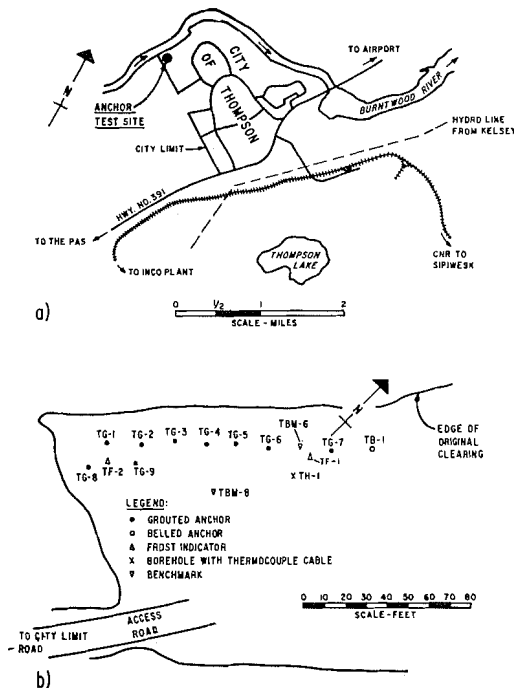


FIG. 2. Thompson - anchor test site.

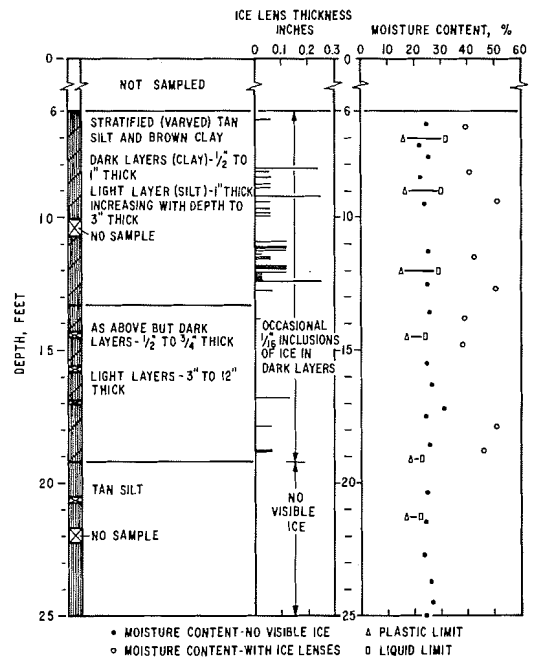


FIG. 3. Soil conditions - hole TH-1 anchor test site Thompson, Manitoba.

dense silt. A 0.3 to 1.0 ft (.1 to .3 m) layer of moss and organic material (peat) covered the mineral soil.

Envelopes of grain size distribution for the various strata are shown in Fig. 5; the "combined samples" refer to a mixture of

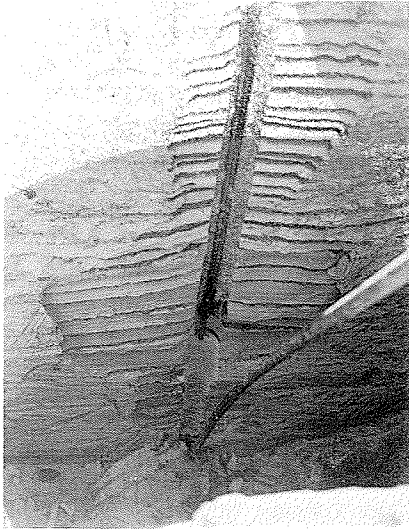


FIG. 4. Soil profile at anchor TG-9, Thompson.

material from light and dark layers. Atterberg limit values are for "combined" samples also. The specific gravity of the silt and clay was 2.76 and 2.80, respectively. The dry density of four samples of silt taken at a depth of 15 ft (4.5 m) from a trench excavated following testing of the anchors ranged from 94.5 to 105.0 lb/ft³ (1512 to 1680 kg/m³) and averaged 98.9 lb/ft³ (1584 kg/m³).

The most significant ice segregation occurred in the top 13 ft (4 m) and was usually associated with the dark layers. Ice lenses were mainly horizontal, although some diagonal or vertical lenses were evident, and varied from hairline to a maximum thickness of about 1/2 in. (1.3 cm); occasional small crystals or nodules of ice were also observed. Very little ice was noted between 13 and 19 ft (4 and 6 m) and none was visible between 19 and 30 ft (6 and 9 m).

Gillam

The surficial geology of the general Gillam area is quite complex. The region was completely glaciated during the Wisconsin and the bedrock is usually mantled with 10 to 100 ft (3 to 30 m) or more of glacial, fluvial

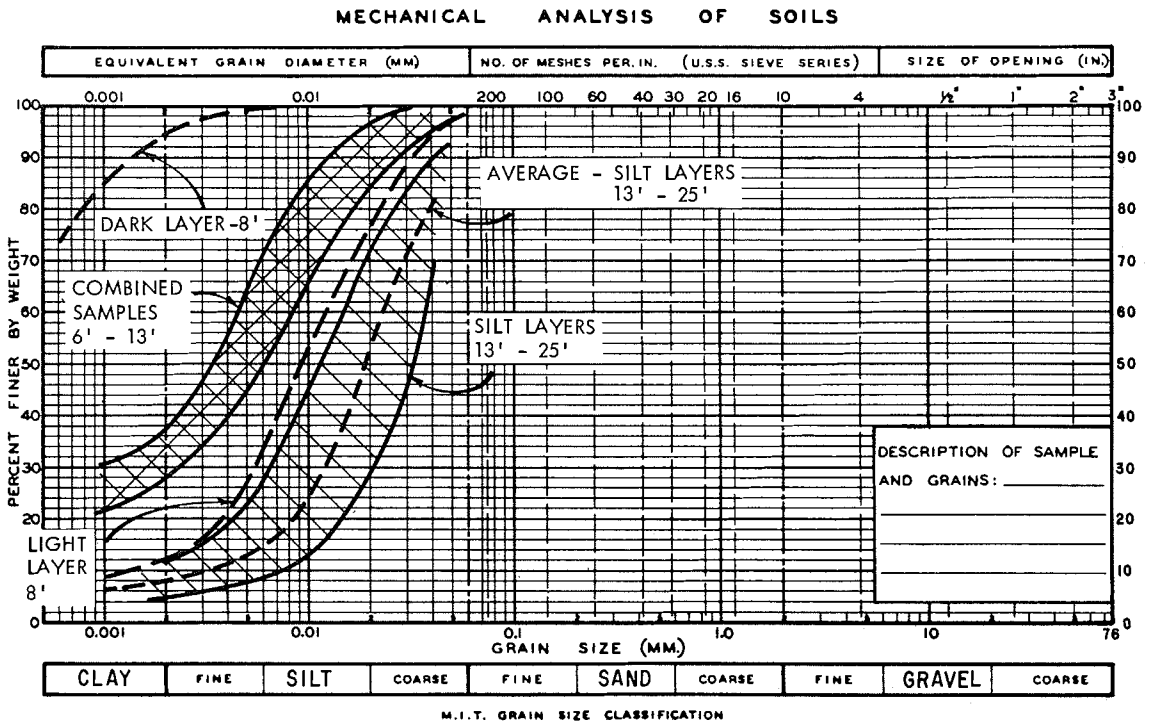


FIG. 5. Grain size envelopes for Thompson soils anchor test site.

and lacustrine materials laid down during and following glaciation, and even with lacustrine deposits resulting from marine encroachment in some areas. Fine sands, silts and clays were deposited as the glaciers receded, particularly in local depressions where a relatively thick organic cover was established.

The Gillam anchor test site is located in a low area about ½ mile (.8 km) SE of the town of Gillam, which is situated on the CNR line to Churchill (Fig. 6). The dense growth of small spruce and underbrush was machine cleared carefully (to keep disturbance of the moss cover to a minimum) in late February 1967 and two 30 ft (9 m) holes (GH-1 and -2) were drilled immediately after the site was cleared (about 160 ft (49 m) apart, one at each end of the line of grouted anchors). From the ground surface to 6 ft (2 m) a 4 in. (10 cm) diameter flight auger was used to penetrate the hard-frozen material; from 6 to 30 ft (2 to 9 m) samples were taken with a 2 in. (5 cm) diameter heavy-wall Shelby tube. A thermocouple cable was installed in hole GH-1 to measure ground temperatures at 2 ft (.6 m) intervals from 2 to 20 ft (.6 to 6 m) and at 25 and 30 ft (7.5 and 9 m).

The site was covered with about 3 ft (1 m) of moss and peat. A brown, faintly laminated, silty clay of medium plasticity changed to a brownish grey to grey silty clay at 14 ft (4 m) in hole GH-1 (Fig. 7) and at 10 ft (3 m) in GH-2. Laminations were somewhat more prominent in the grey silty clay and occasional pebbles and thin sandy and silty layers were observed. The silt content increased with depth (Fig. 8) and the specific gravity of the material was about 2.73.

Ice segregation was significant throughout the profile in both holes and varied from small crystals to lenses ranging from hairline to 4 in. (10 cm) thick (average thickness, approximately ¼ to ½ in. (.6 to 1.2 cm); an occasional ice layer 8 to 9 in. (20 to 23 cm) thick, with thin soil inclusions, was noted. Thicker ice lenses were observed in the grey silty clay below the 12 ft (3.5 m) depth. Soil layers between major ice lenses generally contained no visible ice and were well bonded.

Ground Thermal Regime

At both the Thompson and Gillam sites ground temperatures from about 5 to 30 ft (1.5 to 9 m) were between 31.5 and 31.8 °F,

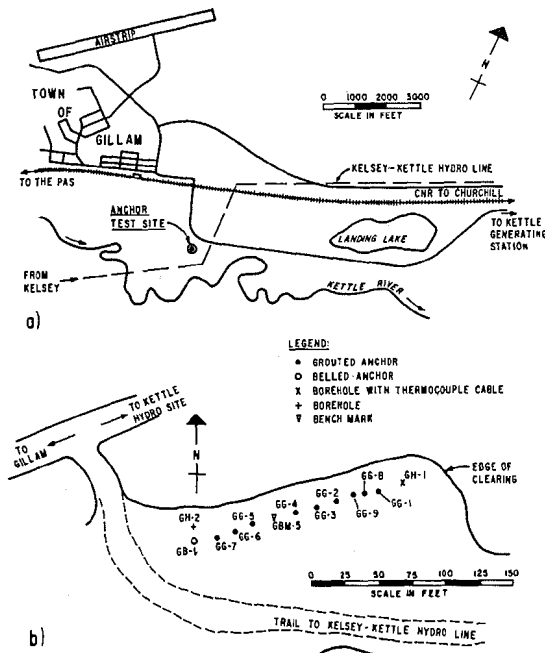


FIG. 6. Gillam - anchor test site.

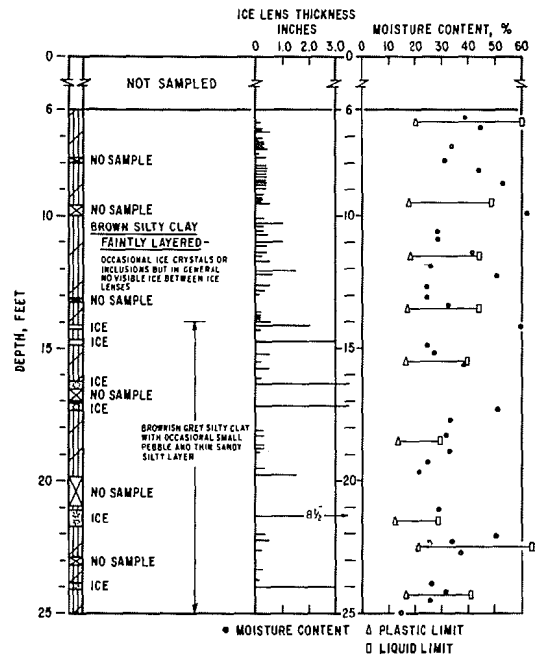


FIG. 7. Soil conditions - hole GH-1 - anchor test site Gillam, Manitoba.

MECHANICAL ANALYSIS OF SOILS

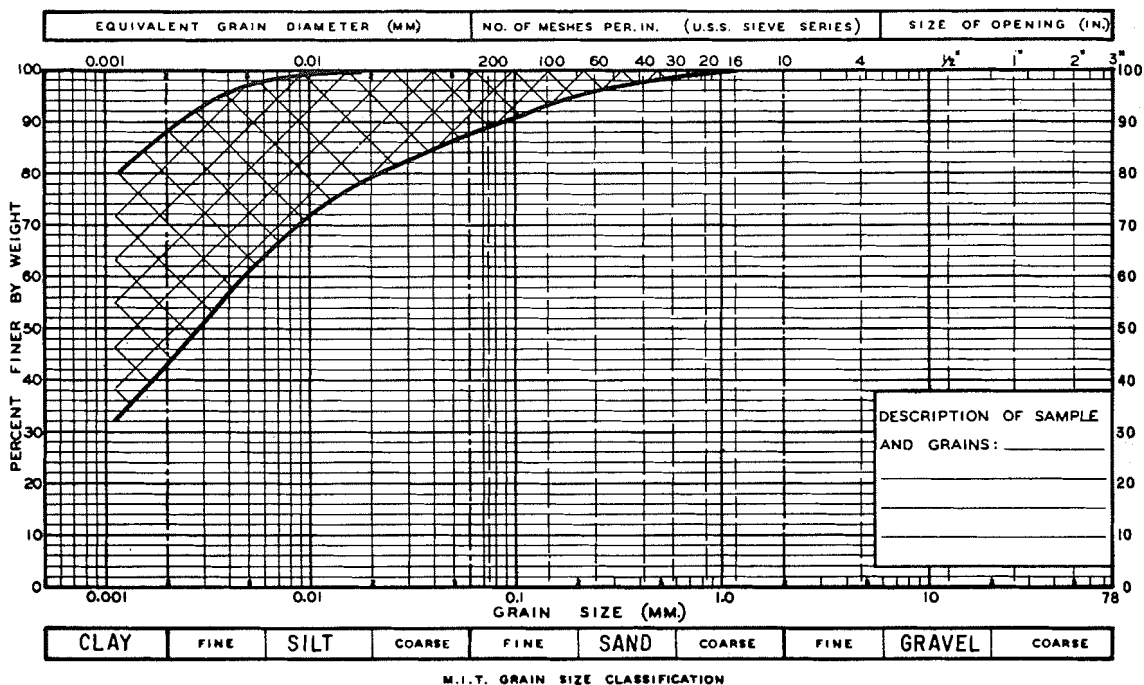


FIG. 8. Grain size envelope for Gillam soils anchor test site II.

i.e., they were essentially isothermal throughout the year. Temperatures in the top 5 ft (1.5 m) varied annually, and their value depended on the time of year.

Prior to clearing, the depth of thaw at the test sites (active layer) ranged from 3 to 4 ft (1 to 1.2 m). Disturbance resulting from removal of some of the organic cover and subsequent testing activity caused an increase. By the time anchor testing was conducted (15 months after installation) the maximum depth of thaw at Gillam was about 4 ft (1.2 m). At Thompson, however, it increased appreciably, reaching a depth of about 8 ft (2.4 m) at some locations 18 months after installation (Fig. 9). Although increased thaw occurred each year, the active layer refroze to the permafrost table each winter by late January.

Degradation of permafrost during the life of a structure as a result of disturbance of the ground thermal regime during construction or other operations in "warm" permafrost areas (*e.g.* the discontinuous zone) is a most important design consideration. In some cases degradation of permafrost cannot be avoided

or prevented and design of foundations and anchors must neglect the frozen soil condition and be based on the thawed condition of the ground (Reinart 1969). This paper, however, is limited to consideration of the behavior of frozen ground at the time of testing the anchors.

Installation of Grouted Anchors

The Thompson anchors were placed between 6 and 14 February 1967 and the Gillam anchors between 8 and 10 March 1967. Air temperatures at both sites during these periods ranged between 0 and -30°F . Details of the grouted anchors are given in Fig. 10.

Similar groups of nine grouted anchors were installed at each of the two test sites. At Thompson, a 6 in. (1.8 m) diameter power auger and at Gillam a Becker Hammer Drill were used to make the holes for the anchors. All were installed vertically, each consisting of a #14S deformed steel reinforcing bar placed in 6 in. (15 cm) nominal-diameter holes partially filled with grout. The grouted length varied from about 8.5 to 10.5 ft (2.5 to 3 m). Six of the anchors in

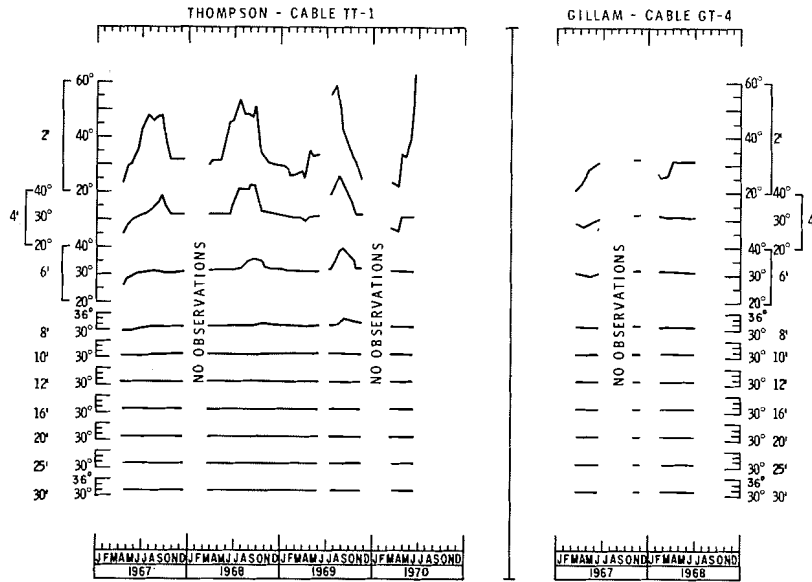


FIG. 9. Ground temperatures - anchor test sites.

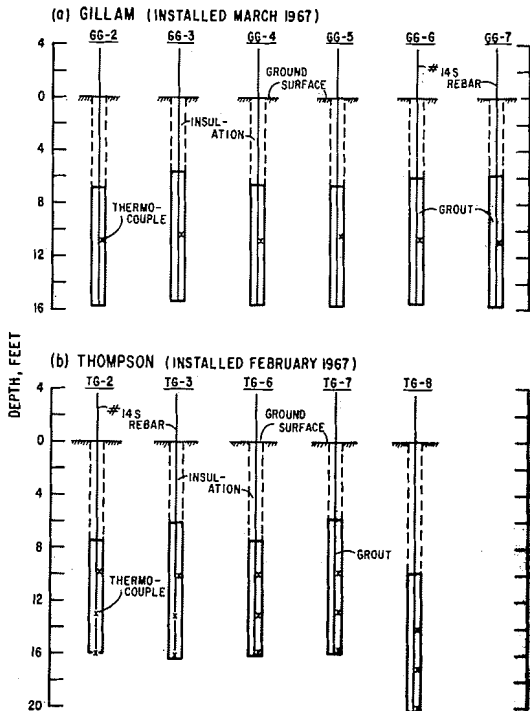


FIG. 10. Grouted anchors - Thompson and Gillam, Manitoba.

each group were placed in holes 16 ft (5 m) deep and the other three were placed in holes 12, 20, and 24 ft (3.5, 6, and 7 m) deep.

The grout was mixed in the proportion of one part cement to one part sand to one half part water (1:1:½). A high early-strength cement (Ciment Fondu) and a clean medium-to-coarse sand were used in all mixes. The water and sand were heated prior to mixing in a small, gasoline engine-driven mixer (the grout for five anchors at Gillam was mixed by hand when the mixer broke down) and the grout was tremied into the hole immediately after it was mixed. Grout temperature, when placed, was between 40 and 55 °F.

Thermocouples were taped to a wooden dowel inserted in the grout midway between the anchor rod and the wall of the hole to measure temperatures at approximately the 1/3, 1/2, 2/3 points and/or the bottom of the grout cylinder. Loose fill insulation (Zonolite or Vermiculite) was poured into the hole between the ground surface and the top of the grout to reduce or eliminate frost heave and air temperature effects.

Test Equipment, Procedures, and Results

Loads were applied to the anchors using 100 ton (90 t) nominal capacity, center-hole hydraulic jacks with 3 in. (5 cm) travel. The jack was placed on top of the collar of a specially designed tubular tripod test frame with a design capacity of about 40 tons (36 t). The

tripod legs were supported by suitable timbers to transfer the load to the surface of the ground. The hydraulic jack was placed over the anchor rod and the load applied to a heavy nut on the threaded upper portion of the rod. The test arrangement is shown in Fig. 11.

As loads were to be maintained for periods varying from $\frac{1}{2}$ hr to several hours or days, the hydraulic system was pressurized by an air-actuated pump. An accumulator was placed in series with the pump to dampen pressure fluctuations in the system. Air for the pump was provided by a gasoline engine-driven compressor and the accumulator was charged with bottled nitrogen. Occasionally, when small loads were applied for short periods of time, a hand-operated pump was used to pressurize the hydraulic system.

Movements of the anchor under test were monitored using an engineer's level. Stainless steel rules graduated in hundredths of an inch were mounted on wood blocks securely attached by U-clamps to the anchor rod and the benchmark. The benchmark was either another stable anchor rod or a specially installed deep benchmark (Bozozuk *et al.* 1963).

One of the anchors for each group of six anchors installed to a depth of 16 ft (5 m) at each of the test sites was first subjected to a fairly large load of about 38 tons (34 t) in order to obtain a representative creep curve. Based on the results of this initial test and on an estimate of the size (surface area and length) of the remaining anchors, each was tested at a smaller but different load.

The other anchors at the sites, placed to different depths, were tested at various loads (less than the maximum used in the first series).

Most of the anchors were tested by applying and maintaining a constant axial load until failure occurred. One anchor (TG-8) was stage-loaded, that is, loads were applied in increments of 3 or 5 kips (1.4 or 2.3 t), each load increment being maintained until a constant rate of strain was obtained. The load selected for each anchor was applied as quickly as possible. Usually, much of the 3 in. (5 cm) jack travel was used up because of settlement of the bearing timbers and adjustment of the bolted test frame. The load was then released entirely, the jack cylinder returned to its initial position, and the load reapplied. This cycle normally took from 3 to 8 min. Occasionally, and particularly during the course of a long test, the jack would also have to be "recycled" as anchor movements increased. Otherwise the load, once applied, was maintained. Recycling of an anchor was required no more than twice during any test.

Upon completion of the test program all grouted anchors at both sites were salvaged (either by excavation or by jacking out of the ground) and their dimensions were measured. Although many of the anchors were removed from the ground intact, a number broke when they were being extracted or when struck by the back-hoe or crane. The typical shape of both the Thompson and Gillam anchors can be seen in Fig. 12, which shows several of the Thompson anchors. The corrugated

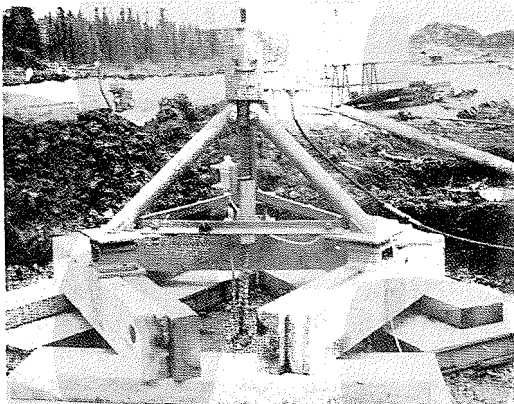


FIG. 11. Grouted anchor under load, Gillam.



FIG. 12. Grouted anchors, Thompson.

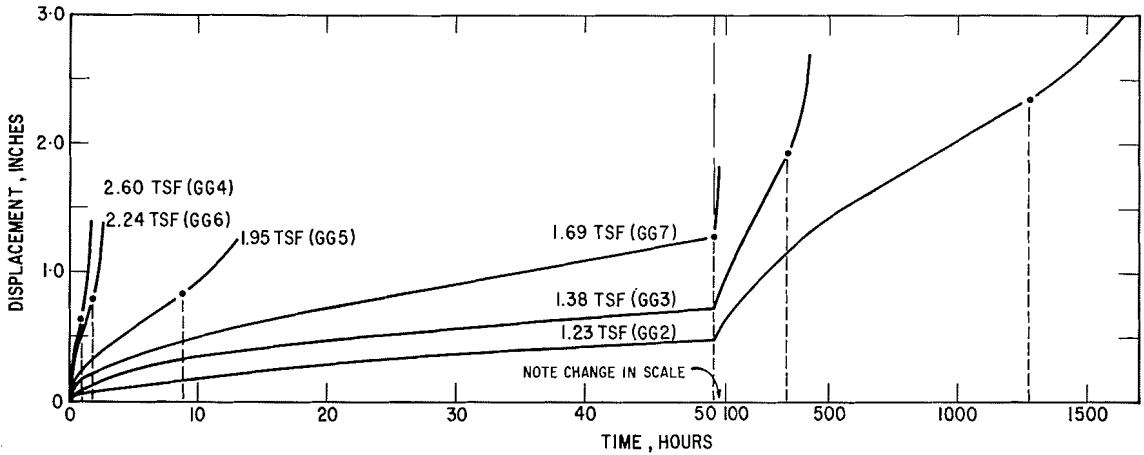


FIG. 13. Sustained-load pull-out tests at Gillam.

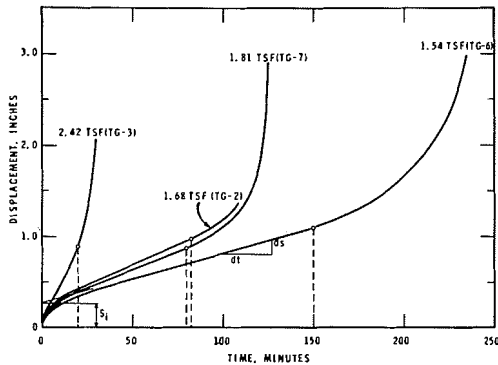


FIG. 14. Sustained-load pull-out tests at Thompson.

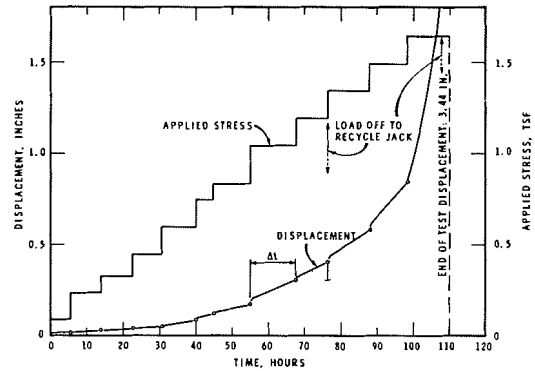


FIG. 15. Stage-loaded anchor test (TG-8) at Thompson.

surface on the Thompson anchors was caused by the marks left by the auger on the wall of the hole. At Gillam, where ice lenses were more extensive and much thicker than at Thompson, it was noted in a test pit excavated beside anchor GG-7 that the corrugations occurred at ice lens locations and therefore probably resulted from thawing of the ice immediately following placement and during curing of the grout.

The placement of a cement grout in a frozen environment can affect the bond between the anchor rod and the grout, the bond between the soil and the grout, and the strength of the grout itself. Quick freezing may not allow the grout to set and cure properly and its strength will be mainly dependent on the strength of the ice cementing the grout particles. Close examination of the grouted anchors following testing indicated

excellent bond and no slip between the anchor rod and the grout; it also indicated that the surface of the grout in contact with the soil was quite firm and not flaky or powdery. The grout itself was hard and the particles were well bonded.

The results of sustained load testing of six anchors at Gillam and four anchors at Thompson are presented as creep curves (displacement vs time) in Figs. 13 and 14 respectively. The bottom of each anchor was at a depth of about 16 ft (4.9 m). The displacement-time curve for Thompson anchor TG-8 (bottom at 20 ft (6.1 m)), which was stage-loaded, is shown in Fig. 15. Pertinent details of the anchors and tests are given in Table 1. Seven anchors, four at Thompson and three at Gillam, of the 18 originally installed were

TABLE 1 Grouted anchors

Anchor Number	Test Date	Length (ft)	Surface Area (ft ²)	Load (tons)	Unit Stress (TSF)	Total Test Time (hr)
<i>Thompson</i>						
TG-2	20.10-21.10/69	8.5	12.8	21.5	1.68	1.75
TG-3	5.6.69	10.2	15.7	38	2.42	0.62
TG-6	1.6.70	8.7	12.4	19	1.54	3.9
TG-7	9.6.69	10.2	15.2	27.5	1.81	2.1
TG-8	27.5-1.6/70	10.3	15.5	1.5-27.5	0.097-1.78	109.7
<i>Gillam</i>						
GG-2	15.7-16.9/68	8.9	14.3	17.5	1.23	1483.3
GG-3	16.7-2.8/68	10.2	16.3	22.5	1.38	403.4
GG-4	10.7.68	9.0	14.4	37.5	2.60	2.0
GG-5	11.7.68	8.8	14.1	27.5	1.95	14.0
GG-6	26.7.68	9.5	15.2	34	2.24	2.7
GG-7	30.7-2.8/68	9.6	15.4	26	1.69	76.5

tested for periods ranging from several hours to more than a year (different load application systems were used for the very long tests), but these results have not been included because they were influenced by deep thawing or difficulties experienced during testing.

Discussion of Results

As may be seen in Figs. 13 and 14, grouted anchors embedded in frozen soil and under sustained load showed typical creep behavior with distinct primary, secondary and tertiary creep stages. The secondary stage is usually very short at higher loads, but it becomes more and more important at lower loads. At very low loads, when the applied shear stress is close to the long-term adfreeze strength, the creep curve often does not go beyond the secondary stage. Nevertheless, if the secondary stage is present, even at such relatively low applied stresses, the third or accelerating stage of creep may take place after a sufficient interval of time and the anchor may fail. It is clear that for design purposes accelerated creep cannot be tolerated. A proper knowledge of the onset of tertiary creep, which in the present case coincides with the beginning of slip between the anchor and the soil, is therefore very important.

From observations of the anchors *in situ* after failure (from trenches excavated immediately adjacent to them) it was evident that deformations round the anchors were

of two kinds: a very thin zone of high shear strain at the soil-grout interface, and an outer zone of uniform shear strain that decreased rapidly with distance from the anchor (Fig. 16). It is considered that the former is a result of slip failure at the anchor-soil interface, coinciding with the region of tertiary creep and failure, while the latter is due to the pre-slip deformation of the soil occurring during primary and secondary creep stages observed in the anchor tests.

As may be seen in Figs. 13, 14, and 15, the onset of the third stage of creep occurred at very different times under different loads, although the total displacements associated with it were of the same order of magnitude

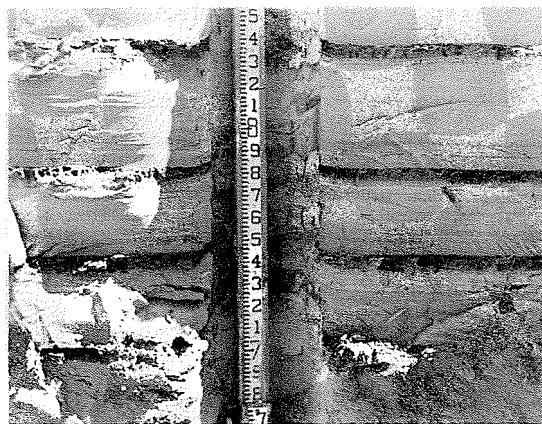


FIG. 16. Section showing slip surface and soil deformation immediately adjacent to grouted anchor, Thompson.

for all the tests. Displacements tended to be of the order of 0.6 to 1.0 in. (1.3 to 2.5 cm) at relatively high loads and to increase with decreasing loads, being about 2.35 in. (6 cm) at the lowest applied sustained load (GG-2, Fig. 13). This observation may help in determining the design load for a grouted rod anchor or a tension pile. For example, the design load may be taken so low that within the lifetime of the structure the total displacement will not attain the displacement associated with the onset of tertiary creep. One approach to determining the design load, based on a criterion of allowable displacement, is described in the following sections.

Theoretical Interpretation of Test Results

Grouted anchors installed as described are essentially similar to short, small-diameter, cast-*in-situ* concrete piles. Their behavior under load is comparable to that of anchor piles in either unfrozen or frozen soils, all of which show usually instantaneous and creep displacements at low loads and slip at loads close to failure. Although creep displacements can be observed in both types of soils their importance in the total displacement of the pile is usually much greater in frozen soils and has to be taken into account in design. Moreover, the behavior of frozen soils is very sensitive to temperature change and therefore temperature becomes an important parameter in design.

The ultimate pulling capacity of cylindrical straight shaft piles in soils can be given by

$$[1] \quad P_{ult} = 2\pi aL\tau_{a\text{ ult}} + W_p$$

where

$$\begin{aligned} P_{ult} &= \text{ultimate pulling capacity,} \\ \tau_{a\text{ ult}} &= \text{ultimate shear strength at} \\ &\quad \text{pile-soil interface,} \\ a &= \text{radius of pile,} \\ L &= \text{embedded length of pile, and} \\ W_p &= \text{effective weight of pile.} \end{aligned}$$

In unfrozen soils the shear strength at the lateral pile surface has been found to depend on soil and groundwater conditions, the type of pile material, and the method of installation. For the short-term case in clays, $\tau_{a\text{ ult}}$ is usually replaced by undrained adhesion, which is usually less than the undrained cohesion of the same soil (Sowa 1970). For

the long-term case, $\tau_{a\text{ ult}}$ is usually expressed by the Coulomb shear strength equation in terms of effective stresses and contains effective adhesion and effective contact skin friction coefficients as parameters (Adams 1969; Meyerhof and Adams 1968; Robinson 1969; Bhatnagar 1969; Sowa 1970).

Equation [1] may also be used for estimating the ultimate pulling capacity of piles in frozen soils. It should be recognized, however, that in such soils the shear strength $\tau_{a\text{ ult}}$ at the lateral surface of the pile is strongly time- and temperature-dependent. Moreover, because piles embedded in frozen soils show important long-term creep displacements under load, it seems more appropriate to determine the design pulling capacity of such piles based on an allowable total displacement or a displacement rate rather than by dividing $\tau_{a\text{ ult}}$ or P_{ult} by a safety factor, as is usually done in unfrozen soils.

Analysis of Pile Displacements

It may be seen in Figs. 13 and 14 that anchors embedded in frozen soil and under a sustained load show typical creep behavior, with distinct primary, secondary and tertiary creep stages. In practice one is mainly concerned with the prediction of displacements in the secondary or steady-state creep stage. This is so because the tertiary stage is usually considered to be beyond the point of creep failure, while the primary stage represents, for long time intervals, only a small portion of the total time. For long time intervals any point on the secondary creep line may, therefore, be given by the following equation (Fig. 14, Test TG-6).

$$[2] \quad s(t) = s_i + \dot{s}t$$

where

$$\begin{aligned} s(t) &= \text{time-dependent displacement} \\ s_i &= \text{pseudo-instantaneous displacement, as shown in Fig.} \\ &\quad \text{14, Test TG-6,} \\ \dot{s} &= ds/dt = \text{steady-state displacement rate, and} \\ t &= \text{time.} \end{aligned}$$

At a given frozen soil temperature both s_i and \dot{s} are functions of the applied shear stress

$$[3] \quad s_i = F(\tau_a)$$

$$[4] \quad \dot{s} = G(\tau_a)$$

Once the functions F and G have been experimentally determined, the displacement of a pile under a sustained load can be determined from eq. [2].

If the pile is loaded by a series of increasing step loads, as in Fig. 15, the displacement at a given time may be evaluated from

$$[5] \quad s(t) = F(\tau_a) + \sum_0^t G(\tau_a) \Delta t$$

In the following it will be shown how the two functions F and G can be evaluated and related to frozen soil properties. It will be assumed that

- (a) the pile is cylindrical in shape,
- (b) the shear stress is uniformly distributed over the pile length embedded in frozen soil,
- (c) the frozen soil is uniform and at constant temperature over the embedded pile length,
- (d) the gravity forces can be disregarded in the analysis.

The foregoing four assumptions have been made to give a simple closed-form solution of the problem. Some are clearly restrictive, however, and comments on their implications seem necessary.

As far as assumption (b) is concerned, measurements made during actual pull-out test and performed on piles in frozen soils (e.g., Voitkovskiy 1968) show that shear stress distribution along the pile varies with load level and time. It is triangular at low loads, with its maximum at the top of the embedded pile length, and becomes more uniform with increasing load level and load duration. The observed initial triangular stress distribution can be attributed to pile deformability, resulting in shear displacements (and corresponding mobilized shear stresses) having maximum values at the top and decreasing with depth eventually to zero at some level within the embedded pile length.

On the other hand, in a uniform soil it can be expected that, for equal shear displacements or displacement rates, equal amounts of shear strength will be mobilized and the resulting stress distribution will be uniform. There are essentially three cases in which equal displacements along the pile, and therefore

the uniform stress distribution assumed in (b), can be expected to occur in practice: (1) when the pile is much less deformable than the soil, (2) when, after a long time interval, initially non-uniform displacements at the pile-soil interface equalize because of relaxation of stresses in the soil, and (3) after slip has occurred.

It follows that before slip occurs the analysis, as shown in the paper, is valid for either short rigid piles at relatively short time intervals or normal anchor piles at long time intervals, for which it was intended. There is, however, no difficulty in extending the analysis to cover also a triangular stress distribution, as will be shown later.

Assumption (c) implies, in turn, that the strength (or creep) behavior of frozen soil is uniform over the embedded pile length. The analysis, as shown, is therefore valid for a pile embedded in a relatively homogeneous layer and with a relatively short embedment, so that average effects of temperature and normal pressure on the soil behavior within the layer can be used in the analysis. There is no difficulty in extending the same analysis to the case where either the soil properties or the soil temperature vary along the embedded pile length, as will be explained later.

Referring to Fig. 17, it can be shown that for a weightless case the applied shear stress τ_a at the pile surface is related to the shear stress at any radial distance r by (Nadai 1963),

$$[6] \quad \tau = (\tau_a) a/r$$

where, in accordance with eq. [1] and assumption (b),

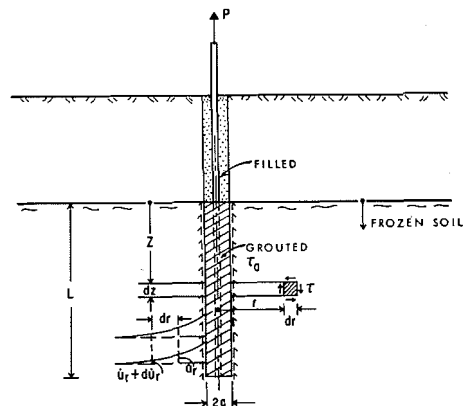


FIG. 17. Definition of terms used in the analysis.

$$[7] \quad \tau_a = (P - W_p)/2\pi aL$$

P is the applied pull load and L the embedded length of pile. If \dot{u} on the other hand, denotes vertical displacement velocity of a particle at radius r , the corresponding rate of shear distortion is given by

$$[8] \quad \dot{\gamma} = -d\dot{u}/dr$$

In order to solve the problem it is necessary to introduce a stress-strain rate relation or a creep law of a general form

$$[9] \quad \dot{\gamma} = f(\tau, T)$$

where τ is the shear stress and T , temperature. One of the simplest forms of such a relation and one that has been extensively used in nonlinear viscoelastic materials such as high-temperature metals and frozen soils is the power creep law (Vialov 1959; Nadai 1963; Odquist 1966; Hult 1966)

$$[10] \quad \dot{\gamma} = \dot{\gamma}_c \left(\frac{\tau}{\tau_c} \right)^n$$

in which τ_c and n are creep parameters determined experimentally and $\dot{\gamma}_c$ is an arbitrary strain rate introduced into eq. [10] to give it a normalized form.

Substituting eqs. (6) and (8) in eq. (10) gives

$$[11] \quad \frac{d\dot{u}}{dr} = -\dot{\gamma}_c \left(\frac{\tau_a a}{\tau_c r} \right)^n$$

Integrating, and noting that at $r = a$, $\dot{u} = \dot{u}_a$, yields

$$[12] \quad \dot{u}_a - \dot{u} = \frac{\dot{\gamma}_c a}{n-1} \left(\frac{\tau_a}{\tau_c} \right)^n \left[1 - \left(\frac{a}{r} \right)^{n-1} \right]$$

As \dot{u} tends to zero when r tends to infinity, the displacement rate of the soil at the contact with the pile is

$$[13] \quad \dot{u}_a = \frac{\dot{\gamma}_c a}{n-1} \left(\frac{\tau_a}{\tau_c} \right)^n$$

If there is no slip between the pile and the soil

$$\dot{u}_a = \dot{s} = G(\tau_a)$$

Thus

$$[14] \quad \dot{s} = G(\tau_a) = \frac{\dot{\gamma}_c a}{n-1} \left(\frac{\tau_a}{\tau_c} \right)^n$$

A completely analogous analysis could be made for finding the pseudo-instantaneous displacement if it is assumed that it has a power law dependence on the stress (as was found for stage loaded tests at Thompson), *i.e.*,

$$[15] \quad \gamma_i = \gamma_k (\tau/\tau_k)^k$$

The resulting displacement may, by analogy with eq. (14), be given by

$$[16] \quad s_i = F(\tau_a) = \frac{\gamma_k a}{k-1} \left(\frac{\tau_a}{\tau_k} \right)^k$$

in which τ_k and k are experimental parameters and γ_k is an arbitrary shear strain. Substituting eqs. [14] and [16] in eq. [5] gives

$$[17] \quad s(t) = s_k \left(\frac{\tau_a}{\tau_k} \right)^k + \sum_0^t \dot{s}_c \left(\frac{\tau_a}{\tau_c} \right)^n \Delta t$$

where s_k and s_c denote, respectively,

$$[18] \quad s_k = \gamma_k a / k - 1$$

$$[19] \quad \dot{s}_c = \frac{\dot{\gamma}_c a}{n-1}$$

The four experimental parameters k , τ_k , n , τ_c in eq. [17] can be obtained by plotting pseudo-instantaneous displacements and steady-state creep rates, respectively, versus the applied stress in a log-log plot. Fig. (18) shows such a plot for creep rates observed in pull-out tests at the Gillam and Thompson test sites. For example, the Gillam test series gives

$$k = 3, \tau_k = 0.571 \text{ TSF (for } s_k = 0.1 \text{ in.)}$$

$$n = 8.05, \tau_c = 1.1535 \text{ TSF (for } \dot{s}_c = 0.001 \text{ in./hr)}$$

the Thompson test series gives

$$k = 3, \tau_k = 0.571 \text{ TSF (for } s_k = 0.01 \text{ in.)}$$

$$n = 7.5, \tau_c = 0.7858 \text{ TSF (for } \dot{s}_c = 0.001 \text{ in./hr)}$$

It should be noted that the foregoing values of parameters k and τ_k represent average values for anchor tests on both sites, τ_k showing a total deviation of ± 0.270 TSF from the mean.

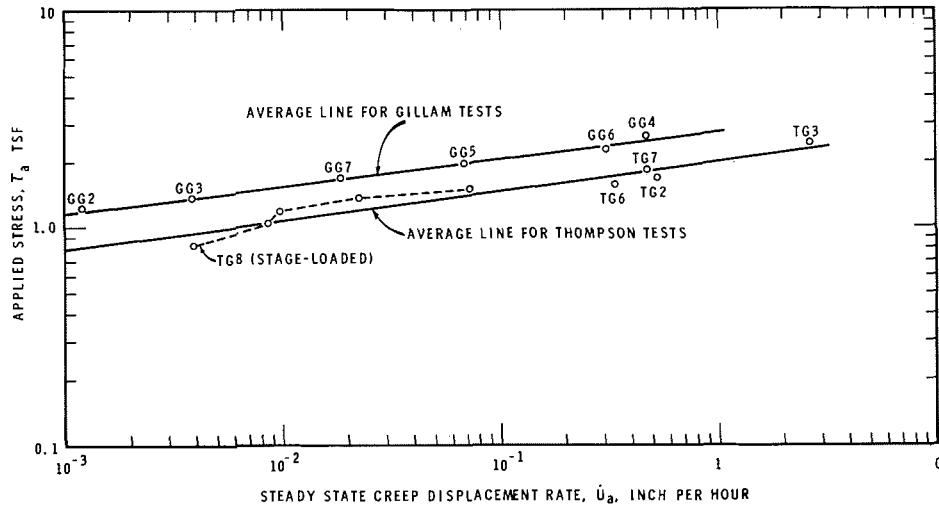


FIG. 18. Steady state creep rate vs average applied shear stress in anchor pull-out tests.

The corresponding creep equations are:

for Gillam ($a = 3.1$ in.),

$$[20] \quad \dot{\gamma} = 2.275 \times 10^{-3} (0.866 \tau_a)^{8.05}$$

for Thompson ($a = 2.8$ in.),

$$[21] \quad \dot{\gamma} = 2.32 \times 10^{-3} (1.271 \tau_a)^{7.5}$$

where $\dot{\gamma}$ is in hours⁻¹ and τ_a in TSF.

The foregoing analysis shows how the time-dependent displacement of the pile is related to average creep properties of frozen soil. It is clear, however, that the deduced creep equations are valid only for simple shear and for the particular normal pressure and temperature in the test. It may, therefore, be of interest to show how the simple shear creep equation may be deduced from the general creep equation.

For a general state of stress and an incompressible von Mises material the power type creep equation can be written as (Odquist 1966).

$$[22] \quad \dot{\epsilon}_c = \dot{\epsilon}_c \left(\frac{\sigma_c}{\sigma_{cu\theta}} \right)^n$$

in which σ_c and $\dot{\epsilon}_c$ are the equivalent stress and strain rate, respectively, defined by

$$[23] \quad \sigma_c^2 = 3 J'_2 = \frac{1}{2} [(\sigma_1 - \sigma_2)^2 + (\sigma_2 - \sigma_3)^2 + (\sigma_3 - \sigma_1)^2]$$

$$[24] \quad \dot{\epsilon}_c^2 = \frac{4}{3} I'_2 = \frac{2}{9} [(\dot{\epsilon}_1 - \dot{\epsilon}_2)^2 + (\dot{\epsilon}_2 - \dot{\epsilon}_3)^2 + (\dot{\epsilon}_3 - \dot{\epsilon}_1)^2]$$

where J'_2 and I'_2 denote second invariants of stress and strain rate deviation tensor, respectively, and $\sigma_{cu\theta}$ is the creep proof stress (creep modulus) obtained in uniaxial compression creep tests at a constant temperature θ .

The temperature dependence of the proof stress $\sigma_{cu\theta}$ can be given by

$$[25] \quad \sigma_{cu\theta} = \sigma_{cu0} f(\theta)$$

where σ_{cu0} is the value of $\sigma_{cu\theta}$ at 0 °C and $f(\theta)$ is a temperature function that may be deduced, *e.g.*, from the theory of rate processes (Andersland and AlNouri 1970; Ladanyi 1972).

$$[26] \quad f(\theta) = \exp \left[\frac{\theta(U/R)}{273 n (273 - \theta)} \right]$$

In eq. [26] θ is the absolute value of negative temperature in degrees centigrade, n is the creep exponent, U is the apparent activation energy of the frozen soil, and $R = 1.987$ cal/mole °C is the universal gas constant. The ratio U/R has the units of temperature; some typical values include: for frozen saturated Ottawa sand ($\gamma_d = 107.5$ p.c.f. (1720 kg/m³) $w = 19.3\%$) (Andersland and AlNouri 1970), $U/R = 4274$ °C; for frozen Sault Ste. Marie clay ($\gamma_d = 98.1$ p.c.f. (1568 kg/m³), $w = 26\%$) (Akili 1970), $U/R = 56\,500$ °C; for polycrystalline ice (Gold 1970), $U/R = 10\,000$ °C.

For a cylindrical symmetry case, as in a triaxial test

$$(\sigma_1 > \sigma_2 = \sigma_3), (\dot{\epsilon}_2 = \dot{\epsilon}_3 = -\dot{\epsilon}_1/2)$$

and eq. [22] becomes

$$[27] \quad \dot{\epsilon}_1 = \dot{\epsilon}_c \left(\frac{\sigma_1 - \sigma_3}{\sigma_{cu\theta}} \right)^n$$

For a plane strain case, in turn,

$$[\sigma_1, \sigma_2 = \frac{1}{2}(\sigma_1 + \sigma_3), \sigma_3], (\dot{\epsilon}_1, \dot{\epsilon}_2 = 0, \dot{\epsilon}_3 = -\dot{\epsilon}_1)$$

and eq. [22] yields

$$[28] \quad \dot{\epsilon}_1 = \left(\frac{\sqrt{3}}{2} \right)^{n+1} \dot{\epsilon}_c \left(\frac{\sigma_1 - \sigma_3}{\sigma_{cu\theta}} \right)^n$$

Finally, for a simple shear case one can write for an incompressible material

$$[29] \quad \tau = \frac{1}{2}(\sigma_1 - \sigma_3)$$

$$[30] \quad \dot{\gamma} = 2\dot{\epsilon}_1$$

and eq. [28] becomes

$$[31] \quad \dot{\gamma} = 3^{(n+1)/2} \dot{\epsilon}_c (\tau/\sigma_{cu\theta})^n$$

Comparing eqs. [31] and [10], one finds that if

$$\sigma_{cu\theta} = \tau_c$$

then

$$[32] \quad \dot{\epsilon}_c = 3^{-(n+1)/2} \dot{\gamma}_c$$

Equation [32] would give

$$\text{for Gillam } \dot{\epsilon}_c = 1.574 \times 10^{-5} \text{ h}^{-1}$$

$$\text{for Thompson } \dot{\epsilon}_c = 2.18 \times 10^{-5} \text{ h}^{-1}.$$

Thus general creep equations in the form of eq. [22] can be written for the two sites.

Effect of Mean Normal Pressure

In the foregoing analysis it has been assumed that frozen soil behaves as a frictionless von Mises material; this would correspond well with a frozen, saturated clay or pure ice. The creep of a frictional frozen soil such as frozen silt or sand can be described by an extended von Mises form in which the effect of hydrostatic pressure has been included. There are several ways of doing this (Vialov 1959; Ladanyi 1972), but a form that seems most convenient for solving the problem at hand is

$$[33] \quad \dot{\epsilon}_c = \dot{\epsilon}_c \left[\frac{(\lambda + 1) \sigma_c}{2\sigma_{cu\theta} + 3(\lambda - 1)\sigma_m} \right]^n$$

in which λ denotes the ratio of uniaxial compressive to uniaxial tensile strength of frozen soil, at a strain rate $\dot{\epsilon}_c = \dot{\epsilon}_c$, usually only little affected by temperature; σ_m is the mean normal (octahedral) pressure; and other symbols are defined as before. For any given set of strain rate, mean normal pressure and temperature, eq. [33] represents a right circular conical surface in the principal stress space.

In terms of shear strength parameters eq. [33] implies that both cohesion and internal friction tend to zero when the strain rate tends to zero. It may be seen that eq. [33] reduces to eq. [22] when $\lambda = 1$, as expected.

Assuming plane strain and constant volume, eq. [33] becomes

$$[34] \quad \dot{\epsilon}_1 = \left(\frac{\sqrt{3}}{2} \right)^{n+1}$$

$$\dot{\epsilon}_c \left[\frac{(\lambda + 1)(\sigma_1 - \sigma_3)}{2\sigma_{cu\theta} + 1.5(\lambda - 1)(\sigma_1 + \sigma_3)} \right]^n$$

In simple shear it is often assumed that directions of maximum shear stress and maximum shear strain rate coincide, as pointed out by Hill (1950). Equations [29] and [30] then remain valid for transforming normal stresses and strains into their shear counterparts. If, moreover, it is assumed that the average mean normal pressure σ_m round the embedded pile length during creep remains constant and equal to the average original ground pressure p_0 given by

$$[35] \quad p_0 = \frac{1}{3}(p_v + 2p_h) = \frac{1}{3}p_v(1 + 2K_0)$$

p_v and p_h being the total vertical and horizontal pressures in the ground at the mid-height of the embedded pile length and K_0 the at-rest earth pressure coefficient, eq. [33] for the simple shear condition may be written as

$$[36] \quad \dot{\gamma} = 3^{(n+1)/2} \dot{\epsilon}_c \left[\frac{(\lambda + 1)\tau}{2\sigma_{cu\theta} + 3(\lambda - 1)p_0} \right]^n$$

Writing

$$[37] \quad \tau_c = \frac{1}{\lambda + 1} [2\sigma_{cu\theta} + 3(\lambda - 1)p_0]$$

and using eq. [32], eq. [36] can be written again in the form of eq. [10]. Consequently, under the foregoing assumptions the analysis of anchor pile displacements in frictional frozen soil remains the same as for the frictionless case.

For example, for varved soil at Thompson, where at a depth of 10 ft (3 m) the soil was about 80% silt, one may have, according to Sanger (1968), an angle of internal friction of about 15°, giving $\lambda \approx 1.7$. Furthermore, assuming for the soil a unit weight of 122 lb/ft³ (8052 kg/m³) and $K_0 = 1$, a value $p_0 = 0.61$ TSF is obtained. Finally, as $\tau_c = 0.7858$ TSF, the corresponding value of $\sigma_{cu\theta}$ from eq. [37] is 0.420 TSF. For that case, eq. [36] takes the form

$$\dot{\gamma} = 2.32 \times 10^{-3} \left[\frac{2.7 \tau}{0.84 + 2.1 p_0} \right]^{7.5}$$

enabling the effect of hydrostatic pressure p_0 on the creep behavior of the soil to be estimated.

It must be recognized that the foregoing analysis is valid only before any slip occurs between pile and soil. In the present tests this condition was satisfied up to about 1 in. total displacement of the anchors.

Condition of Slip

In all pull-out tests with piles embedded in both frozen and unfrozen soils it is usually found that after some finite displacement a slip occurs between the pile and the soil so that the pile fails. In frozen soil tests it is considered that the slip condition starts at the onset of the tertiary stage of creep; this is easily recognized on the pile creep curves. It should be noted in Figs. 13, 14, and 15 that in all the tests the slip condition occurred at a total displacement of the order of about 1 to 2 in. (2.5 to 5 cm). As displacement of the pile is directly related to the shear strain at the interface, this means that creep failure of the frozen soil occurred at almost a constant shear strain, an acceptable assumption in frozen soil mechanics. Even if the total displacement of the pile is not considered as a failure criterion, it is nevertheless useful to be able to determine the time required for it to occur. According to Adams and Hayes (1967), for example, the maximum vertical movements that can be tolerated in a rigid

self-supporting transmission line tower are between 1 and 2 in. (2.5 and 5 cm).

From eq. [2], if s_f is the total tolerable or failure displacement, the time to attainment of s_f will be

$$[38] \quad t_f = \frac{s_f - s_i}{\dot{s}}$$

Substituting eqs. [14] and [16] for \dot{s} and s_i ,

$$[39] \quad t_f = \frac{\left[s_f - s_k \left(\frac{\tau_a}{\tau_k} \right)^k \right]}{\dot{s}_c \left[\frac{\tau_a}{\tau_c} \right]^n}$$

where s_k and s_c are given by eqs. [18] and [19].

After a longer period of more than about 2 or 3 days, s_i becomes less than 10% of the total and may be neglected. Eq. [39] simplifies, then, to

$$[40] \quad t_f \approx \frac{s_f}{\dot{s}_c} \left(\frac{\tau_c}{\tau_a} \right)^n$$

Substituting the previously calculated numerical values in eq. (39), the time, in hours, to a total displacement of 1 in. (approximately the time of the onset of slip at a shear stress τ_a in TSF) is given by:

For Gillam tests

$$[41] \quad t_f = \frac{1.0 - 0.01 (1.75 \tau_a)^3}{0.001 (0.866 \tau_a)^{8.05}}$$

For Thompson tests

$$[42] \quad t_f = \frac{1.0 - 0.01 (1.75 \tau_a)^3}{0.001 (1.27 \tau_a)^{7.5}}$$

Figure 19 shows the t_f vs τ_a lines predicted by eqs. [41] and [42]; these compare well with the actually measured times to the onset of slip of the piles. For longer periods eq. [40] also is sufficiently accurate and can be used for finding a design load under which the pile displacement will not exceed a given allowable limit, s_{all} , within a given time period. From eqs. [40] and [7], the allowable pull-load will be

$$[43] \quad P_{all} = 2\pi a L \tau_c \left(\frac{s_{all}}{\dot{s}_c t} \right)^{\frac{1}{n}} + W_p$$

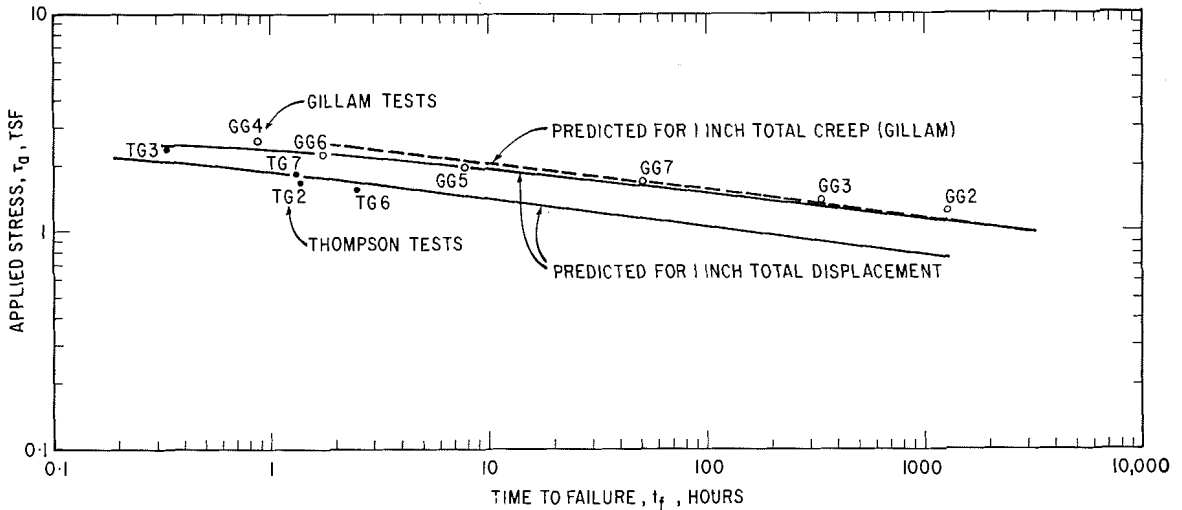


FIG. 19. Time to failure vs average applied shear stress in sustained-load pull-out tests.

This is clearly analogous to eq. [1], but with $\tau_{a \text{ ult}}$ replaced by a $\tau_{a, \text{ all}}$ function of time, temperature, allowable displacement and normal pressure,

$$[44] \tau_{a, \text{ all}} = \frac{1}{\lambda + 1} [2\sigma_{cu\theta} + 3(\lambda - 1) p_0] \left(\frac{s_{\text{all}}}{\dot{s}_c t} \right)^{\frac{1}{n}}$$

For example, for the Gillam site the load under which 1 in. (2.5 cm) creep displacement would be attained after 10 years for a pile of embedded length $L = 10$ ft (3 m) and radius $a = 3.1$ in. (7.5 cm), neglecting its weight W_p , will be, according to eq. [43],

$$P_{\text{all}} = 2\pi a L \tau_{10 \text{ years}} = (16.0 \text{ ft}^2) (0.661 \text{ TSF}) = 10.6 \text{ T.}$$

The same calculation for the data obtained at the Thompson site gives a 10 years' adfreeze strength of 0.432 TSF, and $P_{\text{all}} = 5.75 \text{ T.}$

Effect of Non-Uniform Stress Distribution on Pile Displacement Rate

As mentioned earlier, due to the deformability of the pile the stress distribution along the pile at early stages of loading may be approximately triangular, with its peak value at the top of the embedded length, rather than uniform as assumed in the foregoing analysis. If that is the case, i.e., if the distribution of shear stress τ_a is triangular, with $\tau_a = 0$ at the lower end of the pile, and $\tau_{a \text{ max}}$

$= 2 \tau_{a \text{ average}}$ at the top of the embedded length L , where $\tau_{a \text{ average}}$ is given by eq. [7], the corresponding displacement rate at the top of the pile will be

$$[45] \dot{s} = \dot{s}_c \left[\frac{2\tau_a (\lambda + 1)}{2\sigma_{cu\theta} + 3(\lambda - 1) p_0} \right]^n$$

rather than

$$[46] \dot{s} = \dot{s}_c \left[\frac{\tau_a (\lambda + 1)}{2\sigma_{cu\theta} + 3(\lambda - 1) p_0} \right]^n$$

which is valid for a uniform stress distribution.

Effect of Varying Temperatures on $\tau_{a \text{ all}}$

According to eqs. [25], [26] and [44], $\tau_{a \text{ all}}$ increases with decreasing temperature of the soil. If, therefore, the temperature of an otherwise uniform soil layer varies over the embedded pile length, its response to a given pile displacement rate will be a function of temperature. In this case a simple method can be used to subdivide the total embedded pile length L into a number of sections and take a constant temperature within each section. The value of $\tau_{a \text{ all}}$ can then be calculated for each section (or soil layer) separately. According to eq. [43], the allowable load is then

$$[47] P_{\text{all}} = 2\pi a \sum x_i \tau_{a \text{ all } i} + W_p$$

where $L = \sum x_i$, x_i denoting the thickness of an individual section or soil layer, and

$\tau_{a\text{ all } i}$ the value of $\tau_{a\text{ all}}$ calculated from eq. [44] for a given soil layer, corresponding to its average properties, temperature and normal pressure.

Comparison with Other Experimental Data

Because an independent check of measured creep parameters and adfreeze strengths at the two sites is not yet available, they can only be compared with published experimental data obtained under similar conditions. It is clear that any such comparison is difficult because the behavior of piles in frozen soils depends on a number of factors, some of the most important being the type of pile, the type of frozen soil and its temperature, the method of installation, and the rate of load application. Moreover, at present (1971) there are no data available on the behavior of grouted piles in frozen soils.

Vialov (1959) has performed a large number of full scale loading tests on piles in frozen soils in which he studied the effects of most of the above mentioned factors. For timber piles hand-driven into pre-steamed holes, in both silty sandy loam and argillaceous loam, Vialov (1959, p. 198) gives the following empirical formula for the temperature dependence of the long-term adfreeze strength, τ_{lt} ,

$$[48] \quad \tau_{lt} \text{ (kg/cm}^2\text{)} = \sqrt{1.65 \theta \text{ (}^\circ\text{C)}} - 0.3$$

Vialov also proposes a series of correction factors, taking into account the effect of different soil types and methods of installation. For example, for piles driven by a pile driver into dry-augered holes having a diameter 10 to 40% smaller than the diameter of the pile, he recommends that the τ_{lt} values obtained from eq. [48] be increased by 30 to 50%.

At the Gillam and Thompson sites the permafrost temperature was from 31.5 to 31.8 °F ($\theta = 0.56$ to 0.28 °C), and eq. [48] would therefore give $0.38 > \tau_{lt} > 0.13$ kg/cm². Taking into account that grouting in a pre-drilled hole results in much less disturbance of frozen soil than steaming, assumed by Vialov, the values obtained at the two sites, *i.e.*

$\tau_{10 \text{ years}} = 0.661$ TSF (0.650 kg/cm²) and 0.432 TSF (0.424 kg/cm²) seem reasonable.

On the other hand, Crory (1963) reports on the results of a series of full scale tests carried out in Alaska on 8-in. (20 cm) diameter pipe piles installed in frozen silty sand in dry-augered holes having a diameter about 2 in. (5 cm) greater than the pile. The gap between the pile and the soil was filled with a silt-water slurry ($w = 40$ to 80%). From his Fig. 5 the sustained adfreeze strength of such piles at the temperatures pertinent to the two sites would be,

$$\begin{aligned} \text{at } 31.5 \text{ }^\circ\text{F:} & \quad t_{lt} = 0.28 \text{ TSF,} \\ \text{at } 31.8 \text{ }^\circ\text{F:} & \quad t_{lt} = 0.12 \text{ TSF.} \end{aligned}$$

Again, the values of long-term adfreeze strength at the two sites seem to be of the right order of magnitude.

A more direct check of the reported field data will be possible when the analysis of plate anchor tests conducted at Thompson and Gillam at the same time as the grouted anchor tests has been completed. It is hoped, moreover, that an independent check on frozen soil properties will be obtained from *in situ* frozen soil investigations planned for the Thompson site in 1971.

Conclusions

The field study of grouted pile anchors in permafrost undertaken at two sites in northern Manitoba was designed to investigate the time-dependent behavior of anchors subjected to uplift loads less than those causing rapid failure. The testing program, which consisted of applying constant or step-wise increasing loads for time periods ranging from 1 h to more than a year, enabled all three typical stages of creep displacement to be observed, that is, primary, secondary, and tertiary.

From observations of the piles *in situ* after failure as well as from analysis of the test results it was evident that after a certain amount of creep displacement the piles failed by slip along the soil-pile interface. Slip failure, which was considered to coincide with the onset of tertiary creep, occurred at very different times under different loads, but the total displacement associated with it was of the same order of magnitude for all the tests.

A theoretical analysis of the test results, based on engineering creep theory, shows how

the time-dependent behavior of anchor piles can be related to the basic creep parameters of frozen soil. In addition, it is shown how field creep data may be used for estimating long-term adfreeze strength of frozen soil for the design of anchor piles. The design adfreeze strength is based on a limiting value for the total creep displacement of the anchor pile during its lifetime. The estimated long-term adfreeze strengths computed for the tests described compare well with values obtained by other investigators.

It should be noted that the results presented are for one type of anchor and for rather special materials and conditions, that is, frozen, ice-rich, varved clays and silt at a relatively high temperature of 31.5 to 31.8 °F. As such, they cannot be considered typical. Similar investigations should be carried out to evaluate other soil types and temperatures.

From a practical point of view it is most important that the effects of disturbance on the ground thermal regime (due to construction operations or naturally occurring changes in terrain conditions and climate), which may result in the degradation of permafrost during the life of a structure, be duly considered in the design of foundations and anchors in the discontinuous zone where "warm" permafrost temperatures and a sensitive ground thermal regime are experienced. It should also be noted that the success obtained in the use of grout placed in frozen ground, as reported in this study, may be fortuitous (although great care was taken) and that such results may not always be realized. Great difficulties have been experienced with freezing of concrete or cement grouts when placed in a cold environment; thawing of surrounding frozen ground, which may not refreeze, may also result in such cases and therefore must be considered in the design and construction of foundations in permafrost.

Acknowledgments

J. M. Blackwell, research officer in charge of the DBR Thompson Field Station (TFS) until December 1967, when he left NRC, planned the original program and installed the anchors at both sites. R. D. Stagg, technical officer at TFS, ably assisted during the

planning, installation and testing of anchors at both sites. G. L. Walt, DBR/NRC summer professor during 1968, conducted the anchor tests at Gillam. The authors are most grateful to them for very special efforts under most trying conditions. Special thanks are also extended to I. Reinart, Teshmont Consultants Ltd., and to G. E. McLure, Manitoba Hydro, who provided manpower, materials and equipment assistance at various times during the installation and testing phases. The authors are also indebted to several DBR technical officers who participated at various times in the test program. Many others assisted with or contributed to the program at one time or another, but unfortunately space does not permit an individual acknowledgment to every one. To all, the authors wish to express their sincere thanks.

This paper is a contribution from the Division of Building Research, National Research Council of Canada, and is published with the approval of the Director of the Division.

- ADAMS, J. I. 1969. Grouted-anchor transmission tower footings. *Ont. Hydro Res. Quart.* No. 3, pp. 1-7.
- ADAMS, J. I., and HAYES, D. G. 1967. The uplift capacity of shallow foundations. *Ont. Hydro Res. Quart.*, No. 1, pp. 1-13.
- AKILI, W. 1970. On the stress-creep relationship for a frozen clay soil. *Mater. Res. and Standards*, 10 (1), pp. 16-22.
- ANDERSLAND, O. B., and ALNOURI, I. 1970. Time dependent strength behaviour of frozen soils. *Proc. ASCE*, 96, (SM4) pp. 1249-1265.
- BHATNAGAR, R. S. 1969. Pullout resistance of anchors in silty clay. *Duke Univ., School of Engineering, Soil Mech. Series No. 18.*
- BOZOUK, M., JOHNSTON, G. H., and HAMILTON J. J. 1963. Deep bench marks in clay and permafrost areas, *In Field testing of soils*, ASTM Sp. Tech. Pub. No. 322, p. 265.
- CRORY, F. E. 1966. Pile foundations in permafrost. *Proc. 1st Permafrost Int. Conf., Lafayette, Indiana*, NAS-NRC Publ. No. 1287, pp. 467-472.
- GOLD, L. W. 1970. The failure process in columnar grained ice. Ph.D. Thesis, McGill University, Montreal, Quebec.
- HILL, R. 1950. *The mathematical theory of plasticity.* Oxford, Clarendon Press.
- HULT, J. A. H. 1966. *Creep in engineering structures.* Blaisdell Publ. Co., Waltham, Mass., 115 p.
- JOHNSTON, G. H., BROWN, R. J. E., and PICKERSGILL, D. N. 1963. *Permafrost investigations at Thompson, Manitoba: terrain studies*, National Research Council of Canada, Division of Building Research, NRCC 7568.

- LADANYI, B. 1972. An engineering theory of creep of frozen soil. To be published.
- MEYERHOF, G. G. and ADAMS, J. I. 1968. The ultimate uplift capacity of foundations, *Can. Geotech. J.*, **5**, pp. 225-244.
- NADAI, A. 1963. Theory of flow and fracture of solids, Vol. 2, McGraw-Hill, New York.
- ODQUIST, F. K. G. 1966. Mathematical theory of creep and creep rupture, Oxford Math. Mono., Clarendon Press.
- REINART, I. 1969. Design of foundations for the Nelson River transmission line. Paper presented at the Engineering Institute of Canada, Annual Meeting, Vancouver, B.C.
- ROBINSON, K. E. 1969. Grouted rod and multi-helix anchors, Proc. Spec. Session 14/15, 7th Int. Conf. ISSMFE, Mexico, pp. 126-131.
- SANGER, F. J. 1968. Ground freezing in construction, *Proc. ASCE*, **94** (SM1), pp. 131-158.
- SOWA, V. A. 1970. Pulling capacity of concrete cast *in situ* bored piles, *Can. Geotech. J.*, **7**, pp. 482-493.
- VIALOV, S. S. 1959. Rheological properties and bearing capacity of frozen soils, Transl. 74, U.S. Army CRREL, Hanover, N.H. 1965.
- VOITKOVSKIY, K. F. (Ed.) 1968. Foundations of structures on frozen soils in Yakutia, (in Russian), Nauka Moscow.

This publication is being distributed by the Division of Building Research of the National Research Council of Canada. It should not be reproduced in whole or in part without permission of the original publisher. The Division would be glad to be of assistance in obtaining such permission.

Publications of the Division may be obtained by mailing the appropriate remittance (a Bank, Express, or Post Office Money Order, or a cheque, made payable to the Receiver General of Canada, credit NRC) to the National Research Council of Canada, Ottawa. K1A 0R6. Stamps are not acceptable.

A list of all publications of the Division is available and may be obtained from the Publications Section, Division of Building Research, National Research Council of Canada, Ottawa. K1A 0R6.